УДК 548.534

The Influence of Uniform Pressure on Propagation of Acoustic Waves in Piezoelectric Layered Structures

Sergey I. Burkov*
Institute of Engineering Physics and Radio Electronics,
Siberian Federal University,
Svobodny, 79, Krasnoyarsk, 660041,
Russia

Olga P. Zolotova†
Siberian State Aerospace University,
Krasnoyarsky Rabochy Ave., 31, Krasnoyarsk, 660014,
Russia

Boris P. Sorokin‡
Technological Institute for Superhard and Novel Carbon Materials,
Central'naya, 7a, Troitsk, Moscow, 142190,
Russia

Received 15.08.2013, received in revised form 06.10.2013, accepted 16.11.2013

Basic equations and boundary conditions describing the propagation of acoustic waves in piezoelectric layered structures subjected to uniform pressure have been obtained. The propagation of dispersive acoustic modes in the "[100](001)BGO/fused silica" and "fused silica/[010](100) $LiNbO_3$" layered structures has been analyzed in detail. Selection of solutions identified as the Rayleigh and Love modes of various orders has been fulfilled. Dispersion relations for the phase velocity, EMCC and coefficients α_v in terms of parameter $h \times f$ have been obtained. Anisotropy of acoustic wave parameters in the "(001) BGO/fused silica" structure has been investigated. Directions with the maximum values of the coefficients α_v have been found for some acoustic modes.

PACS: 43.25.Fe; 43.35.Cg; 77.65.-j.

Keywords: piezoelectric layered structure, Love wave, Rayleigh wave, initial stress influence

Introduction

Electronic engineers are now engaged in developing acoustoelectronic devices, such as sensors, filters, resonators et al, for industrial and medical applications. Wave propagation in crystals subjected to external static fields, especially the external uniaxial stress is one the important issues in this field [1, 2]. For example, piezoelectric sensors are commonly used to measure pressures (up to 100-200 MPa/V). They operate on frequencies from 40 kHz to 100 MHz [3]. Internal mechanical stress significantly modifies parameters of piezoelectric devices due to changes in the properties of crystalline material. Changes in physical properties of the crystal subjected to uniform pressure were used in [4, 5] to stabilize the frequency of the resonator, in particular to compensate the frequency shift due to temperature change in langasite or quartz resonators [6, 7]. Changes of surface acoustic wave (SAW) velocity caused by the application of diametric force and bending moment to the langasite and quartz resonators have been analyzed [8]. The contribution

*sburkov@sfu-kras.ru
†dholza@mail.ru
‡bpsorokin2@rambler.ru

of the nonlinear material elastic constants has been analyzed. It has been found that the influence of these constants cannot be ignored for some configurations and it can lead to a significant error in the determination of the resonance frequency shift. General theory of SAW propagation in piezoelectric crystals and theoretical investigation of reflection and refraction of elastic waves on the interface between two elastic media under external pressure has been considered in [9,10].

Such structures as "layer/substrate" (dielectric or piezoelectric layer of finite thickness deposited on a semi-infinite substrate with other material properties) are widely used for the development of acoustoelectronic devices. The effect of initial stress on the Love wave propagation in the "piezoelectric crystal/isotropic substrate" and "isotropic layer/piezoelectric substrate" layered structures has been studied [11, 12]. The effect of uniaxial pressure on the Love wave parameters in a structure consisting of a transversely isotropic piezoelectric substrate and functionally graded material film has been investigated in detail [13]. Let us note that usually cubic, hexagonal and tetragonal crystals are considered as piezoelectric medium.

A complete set of linear and nonlinear material properties of a crystal should be taken into account for the correct analysis.

In this paper we examine the influence of uniform external pressure on the dispersion parameters and on the anisotropy of the Rayleigh and Love waves propagation in the "$Bi_{12}GeO_{20}$/fused silica" and "fused silica/$LiNbO_3$" layered structures.

1. Theory of elastic waves propagation in layered piezoelectric structure subjected to uniform pressure

Let the X_3 axis of orthogonal coordinate system is directed along the outer normal to the surface of the layer, occupying the $0 \leqslant X_3 \leqslant h$ space, and the X_1 axis coincides with the direction of wave propagation. Referring to the initial configuration, the equations of small-amplitude wave propagation, electrostatic equations and state equations for the uniformly deformed acentric crystals under the static pressure can be written in the following form [14]

$$\begin{aligned} &\rho_0 \ddot{\tilde{U}}_A = \tilde{\tau}_{AB,B} + \tilde{U}_{A,PQ}\, \bar{\tau}_{PQ}; \\ &\tilde{D}_{M,M} = 0; \\ &\tilde{\tau}_{AB} = C^*_{ABCD}\, \tilde{\eta}_{CD} - e^*_{MAB} \tilde{E}_M; \\ &\tilde{D}_M = \varepsilon^*_{MN} \tilde{E}_N + e^*_{MAB} \tilde{\eta}_{AB}. \end{aligned} \tag{1}$$

Here the following thermodynamic variables and material tensors are introduced: ρ_0 is the crystalline density referred to undeformed (initial) state, $\tilde{U}_A$ is the unit vector of the dynamic elastic displacement, τ_{AB} is the tensor of thermodynamic stress, η_{AB} is the strain tensor, $\bar{\tau}_{PQ} = -\bar{\tau}\, P_P P_Q$ is the uniaxial stress tensor, P_P is a unit vector of the pressure force and $\tilde{D}_M$ is the vector of electric displacement. In what follows the time-dependent variables are marked by tilde character. The comma after the subscript denotes the spatial derivative and Latin coordinate indices vary from 1 to 3. The rule of summation over repeated indices is used. Effective elastic, piezoelectric and dielectric constants which are the linear functions of pressure $\bar{\tau}$ are defined as follows [15]:

$$\begin{aligned} &C^*_{ABKL} = C^E_{ABKL} - C^E_{ABKLQR}\, S^E_{QRMN} P_M P_N \bar{\tau}; \\ &e^*_{NAB} = e_{NAB} - e_{NABKL}\, S^E_{KLMN} P_M P_N \bar{\tau}; \\ &\varepsilon^*_{MN} = \varepsilon^\eta_{MN} - H_{NMAB}\, S^E_{ABKL} P_K P_L \bar{\tau}. \end{aligned} \tag{2}$$

Here C^E_{ABKL}, e_{NAB} and ε^η_{NM} are the second-order elastic, piezoelectric and clamped dielectric material constants, respectively; S^E_{ABKL} is the tensor of elastic compliance; C^E_{ABKLQR} and e_{NABKL} are the third-order elastic and nonlinear piezoelectric constants, respectively; H_{NMAB} is the tensor of electrostriction.

Let us take solutions for elastic displacements and electrical potential in the form of small-amplitude plane waves. Substituting these solutions into equation (1) and taking into account only the terms which are proportional to pressure, one can obtain the linearized Green-Christoffel equations

$$\begin{array}{l}\left[\Gamma_{BC}\left(P\right)-\rho_0\omega^2\delta_{BC}\right]\tilde{U}_C=0;\\ \Gamma_{BC}=\left[C^*_{ABCD}+\left(2C^E_{MBFN}S^E_{ADCF}+\delta_{BC}\delta_{AM}\delta_{DN}\right)P_MP_N\bar{\tau}\right]k_Ak_D;\\ \Gamma_{C4}=e^*_{PAC}k_Pk_A;\quad \Gamma_{4C}=\Gamma_{C4}+2e_{AFD}S^E_{MNCF}P_MP_N\bar{\tau}k_Ak_D;\quad \Gamma_{44}=-\varepsilon^*_{PQ}k_Pk_Q.\end{array}\tag{3}$$

Here k_A is the wave vector. SAW propagation in a piezoelectric layered structure under the influence of uniform pressure must satisfy the relevant boundary conditions. Firstly, the normal components of the stress tensor at the free surface of the layer should be equal to zero. Secondly, the continuity of the tangential components of the electric field is ensured by the condition of continuity of the electric potential φ at the "layer/vacuum" boundary. In addition, the condition of equality of the normal components of the stress tensor and condition of continuity of the electric potential at the "layer-substrate" interface ($X_3=0$) must be satisfied:

$$\begin{array}{l}\tau^{(2)}_{3A}=0\Big|_{X_3=h};\quad D^{(2)}_3=D^{(vac)}\Big|_{X_3=h};\quad \varphi^{(2)}=\varphi^{(vac)}\big|_{X_3=h};\\ \tau^{(1)}_{3A}=\tau^{(2)}_{3A}\Big|_{X_3=0};\quad D^{(1)}_3=D^{(2)}_3\Big|_{X_3=0};\quad \varphi^{(1)}=\varphi^{(2)}\big|_{X_3=0};\quad U^{(1)}_A=U^{(2)}_A\Big|_{X_3=0}.\end{array}\tag{4}$$

In what follows superscript 1 denotes a substrate and superscript 2 denotes a layer.

If mechanical pressure is imposed orthogonally to the free surface $\left(\vec{P}||X_3\right)$ then elastic properties of the loading medium must be taken into account. Let us assume that a layered structure is in contact with a gas. In this case the mechanical boundary conditions can be written in the form [16]:

$$\tilde{\tau}_{3J}+\tilde{U}_{J,K}\,\bar{\tau}_{3K}=0\quad\left(X_3=0\right).\tag{5}$$

Substituting the solutions in the form of homogeneous plane waves into boundary conditions (4) and taking into account equations (1) and (2) one can obtain the system of equations involving parameters of SAW propagation in a layered piezoelectric structure:

$$\begin{array}{l}\sum\limits_{n=1}^{8}\left[a_n\left(e^{*(2)}_{3AB}+2S^{(2)E}_{ABKP}e^{(2)}_{3AB}P_KP_P\bar{\tau}\right)k^{(n)}_B\alpha^{(n)}_A+a_4\left(\varepsilon^{*(2)}_{3K}k^{(n)}_K-i\varepsilon_0\right)\alpha^{(n)}_4\right]\times\\ \quad\times\exp\left(ik^{(n)}_3h\right)=0;\\ \sum\limits_{n=1}^{8}\left[a_n\left(C^{*(2)}_{B3KL}+2S^{(2)E}_{KPMN}C^{(2)}_{3BKL}P_MP_N\bar{\tau}\right)k^{(n)}_L\alpha^{(n)}_P-a_4e^{*(2)}_{P3B}k^{(n)}_P\alpha^{(n)}_4\right]\times\\ \quad\times\exp\left(ik^{(n)}_3h\right)=0;\\ \sum\limits_{m=1}^{4}b_m\left[\left(C^{*(1)}_{B3KL}+2S^{(1)E}_{KPMN}C^{(1)E}_{3BKL}P_MP_N\bar{\tau}\right)k^{(m)}_L\alpha^{(m)}_P+e^{*(1)}_{P3B}k^{(m)}_P\alpha^{(m)}_4\right]-\\ \quad-\sum\limits_{n=1}^{8}a_n\left[\left(C^{*(2)}_{B3KL}+2S^{(2)E}_{KPMN}C^{(2)E}_{3BKL}P_MP_N\bar{\tau}\right)k^{(n)}_L\alpha^{(n)}_P+e^{*(2)}_{P3B}k^{(n)}_P\alpha^{(n)}_4\right]=0;\\ \sum\limits_{m=1}^{4}b_m\left[\left(e^{*(1)}_{3AB}+2S^{(1)E}_{ABKP}e^{(1)}_{3AB}P_KP_P\bar{\tau}\right)k^{(m)}_B\alpha^{(m)}_A+\varepsilon^{*(1)}_{3K}k^{(m)}_K\alpha^{(m)}_4\right]-\\ \quad-\sum\limits_{n=1}^{8}a_n\left[\left(e^{*(2)}_{3AB}+2S^{(2)E}_{ABKP}e^{(2)}_{3AB}P_KP_P\bar{\tau}\right)k^{(n)}_B\alpha^{(n)}_A+\varepsilon^{*(2)}_{3K}k^{(n)}_K\alpha^{(n)}_4\right]=0;\\ \sum_{m=1}^{4}\left[U^{(1)(m)}_Ib_m\right]-\sum_{n=1}^{8}\left[U^{(2)(n)}_Ia_n\right]=0.\end{array}\tag{6}$$

Here $\alpha^{(n)}_K$, $a^{(n)}$ and $k^{(n)}_L$ are the amplitudes, weight coefficients and wave vectors of the n-th partial wave ($n=1,\ldots,8$) in the layer; $\beta^{(m)}_K$, $b^{(m)}$ and $q^{(m)}_P$ are the amplitudes, weight coefficients

and wave vectors for the m-th partial wave ($m = 1, \ldots, 4$) in the substrate. Let us note that relations (6) take into account all changes in the configuration of an anisotropic continuum, in particular, the changes in the sample's shape (geometric nonlinearity) and the changes in the material constants (2) (physical nonlinearity) under the influence of strong static pressure. Now we have the system of twelve homogeneous equations (6) involving unknown amplitude coefficients a_n and b_m. The standard method of partial waves [17] was used to calculate the elastic wave parameters. By setting the determinant of the boundary condition matrix to zero, we find the SAW phase velocity.

Let us consider the influence of static uniform pressure on the elastic wave propagation in the (001) crystallographic plane of piezoelectric crystal belonging to the (23) cubic symmetry. Uniaxial pressure imposed along the [100] direction changes the initial 23 point symmetry to orthorhombic class 222 according to the Curie principle of symmetry [14]. As a result, the existing material constants are modified:

$$
\begin{aligned}
C^*_{11} &= C^E_{11} + [C_{111}S_{11} + (C_{112} + C_{113})\,S_{12}]\,\bar{\tau};\\
C^*_{33} &= C^E_{11} + [C_{112}S_{11} + (C_{113} + C_{111})\,S_{12}]\,\bar{\tau};\\
C^*_{13} &= C^E_{12} + [C_{113}S_{11} + (C_{123} + C_{112})\,S_{12}]\,\bar{\tau};\\
C^*_{44} &= C^E_{44} + [C_{144}S_{11} + (C_{166} + C_{155})\,S_{12}]\,\bar{\tau};\\
C^*_{55} &= C^E_{44} + [C_{155}S_{11} + (C_{144} + C_{166})\,S_{12}]\,\bar{\tau};\\
C^*_{66} &= C^E_{44} + [C_{166}S_{11} + (C_{155} + C_{144})\,S_{12}]\,\bar{\tau};\\
C^*_{12} &= C^E_{12} + [C_{112}S_{11} + S_{12}(C_{113} + C_{123})]\,\bar{\tau};\\
C^*_{23} &= C^E_{12} + [C_{123}S_{11} + S_{12}(C_{112} + C_{113})]\,\bar{\tau};\\
C^*_{22} &= C^E_{11} + [C_{113}S_{11} + S_{12}(C_{111} + C_{112})]\,\bar{\tau};\\
e^*_{14} &= e_{14} + [e_{114}S_{11} + (e_{124} + e_{134})\,S_{12}]\,\bar{\tau};\\
e^*_{36} &= e_{14} + [e_{124}S_{11} + (e_{134} + e_{114})\,S_{12}]\,\bar{\tau};\\
e^*_{25} &= e_{14} + [e_{134}S_{11} + S_{12}(e_{114} + e_{124})]\,\bar{\tau};\\
\varepsilon^*_{11} &= \varepsilon^\eta_{11} + [H_{11}S_{11} + (H_{12} + H_{13})\,S_{12}]\,\bar{\tau};\\
\varepsilon^*_{33} &= \varepsilon^\eta_{11} + [H_{11}S_{11} + (H_{31} + H_{32})\,S_{12}]\,\bar{\tau}.
\end{aligned}
\tag{7}
$$

Then components of the Green-Christoffel tensor (3), when the static deformation tensor is taken as $\bar{\eta}_{AB} = S_{ABCD}\,\bar{\tau}_{CD}$ [14], can be presented in the form:

$$
\begin{aligned}
\Gamma_{11} &= [C^*_{11} + (2C_{11}S_{11} + 1)\bar{\tau}]\,k_1^2 + (C^*_{55} + 2C_{44}S_{11}\bar{\tau})k_3^2;\\
\Gamma_{13} &= [C^*_{13} + (4C_{44}S_{12} + 1)\bar{\tau} + C^*_{55}]\,k_1k_3;\\
\Gamma_{31} &= [C^*_{13} + 2C_{44}(S_{11} + S_{12})\bar{\tau} + C^*_{55}]\,k_1k_3;\\
\Gamma_{22} &= (C^*_{66} + 2C_{44}S_{12}\bar{\tau})k_1^2 + (C^*_{44} + 2C_{12}S_{12}\bar{\tau})k_3^2;\\
\Gamma_{33} &= (C^*_{55} + 2C_{44}S_{12}\bar{\tau})k_1^2 + (C^*_{33} + 2C_{11}S_{12}\bar{\tau})k_3^2;\\
\Gamma_{24} &= (e^*_{14} + e^*_{36})\,k_1k_3; \quad \Gamma_{42} = (e^*_{14} + e^*_{36} + 4e_{14}S_{12}\bar{\tau})\,k_1k_3;\\
\Gamma_{44} &= \varepsilon^*_{11}k_1^2 + \varepsilon^*_{33}k_3^2.
\end{aligned}
\tag{8}
$$

The application of uniaxial stress along the [100] direction to the (23) point symmetry crystal removes the degeneracy of shear bulk acoustic wave (BAW) velocity. The Green-Christoffel tensor turns asymmetric under static deformation [18].

The application of uniaxial stress to the isotropic medium such as fused silica reduces the initial symmetry to the ∞/mmm Curie group. In terms of elastic properties this symmetry group is similar to the hexagonal symmetry group. As a result, new elastic moduli occur. In particular, when uniaxial pressure is imposed in the direction which coincides with the BAW propagation direction the effective elastic moduli take the following form

$$
\begin{aligned}
C^*_{22} &= C^*_{11} = C^E_{11} + [C_{111}S_{12} + C_{112}(S_{12} + S_{11})]\,\bar{\tau};\\
C^*_{12} &= C^E_{12} + (C_{123}S_{11} + 2C_{112}S_{12})\,\bar{\tau};\\
C^*_{33} &= C^E_{11} + (C_{111}S_{11} + 2C_{112}S_{12})\,bar\tau;\\
C^*_{55} &= C^*_{44} = C^E_{44} + [C_{144}S_{12} + C_{155}(S_{11} + S_{12})]\,\bar{\tau};\\
C^*_{66} &= C^E_{44} + (C_{144}S_{12} + 2C_{155}S_{12})\,\bar{\tau};\\
C^*_{13} &= C^*_{23} = C^E_{12} + [C_{123}S_{12} + C_{112}(S_{12} + S_{11})]\,\bar{\tau}.
\end{aligned}
\tag{9}
$$

In this case, even if the values of phase velocities of longitudinal or shear waves are changed, the degeneracy of shear waves is maintained. However, when acoustic wave propagates along a direction which is orthogonal to the applied pressure the shear wave degeneracy is removed.

2. Dispersive relations and elastic anisotropy of the acoustic wave parameters in layered piezoelectric structures

Taking into account equations (1)–(6), various elastic wave parameters such as phase velocity, electromechanical coupling coefficient (EMCC) and controlling coefficient of phase velocity can be obtained. These parameters are calculated for different order modes of the Rayleigh (R_i) and Love (L_i) waves propagating in layered piezoelectric structures "$Bi_{12}GeO_{20}$/fused silica" and "fused silica/$LiNbO_3$" for a number of options of pressure directions relative to the acoustic wave path. The following variants are considered: (1) pressure acts along the SAW propagation direction, (2) pressure acts in the direction which is orthogonal to the sagittal plane, (3) pressure acts along a normal to the outer surface of the layered structure. For SAW parameter calculations in cubic crystal it is assumed that the locus of propagation directions lies in the (001) plane. In the case of trigonal crystals it is assumed that the locus of propagation directions lies in the (100) and (001) planes.

Let us introduce the controlling coefficient of phase velocities under the action of pressure in the form

$$\alpha^{\tau}_{v} = \frac{1}{v\,(0)}\left(\frac{\Delta v}{\Delta P}\right)_{\Delta P \to 0}. \tag{10}$$

Data for linear and nonlinear electromechanical properties can be found in [19] ($LiNbO_3$ (LN)), [16] ($Bi_{12}GeO_{20}$ (BGO)), and in [20] (fused silica).

The following relation is used to calculate the electromechanical coupling coefficient:

$$K^2 = 2\frac{v - v_m}{v}, \tag{11}$$

where v and v_m are the SAW phase velocities on free surface and metalized surface of the piezoelectric layer, respectively. Because the interdigital trasducers (IDT) can be placed either on the top surface of acoustoelectronic device or under the piezoelectric film on the substrate, the EMCC can be calculated as in the case of upper layer metallization and when metallization is placed between film and substrate.

Figs. 1 and 2 present the dependence of the phase velocity, the EMCC and controlling coefficients for the Rayleigh and Love waves in the investigated layer structures on the $h \times f$ parameter, where h is the thickness of the layer and f is the acoustic wave frequency. As can be seen the action of uniaxial pressure does not result in hybridization of the elastic wave modes in these structures [21, 22].

Dispersion relations for the phase velocity, the EMCC and α_v coefficients for the Rayleigh and Love waves in the "[100](001)BGO/fused silica" structure are presented in Fig. 1. Parameter $h \times f$ is in the range from 0 to 5000 m/s. The Love wave phase velocities lies between the value of the shear wave phase velocity for fused silica and the value of the shear wave phase velocity

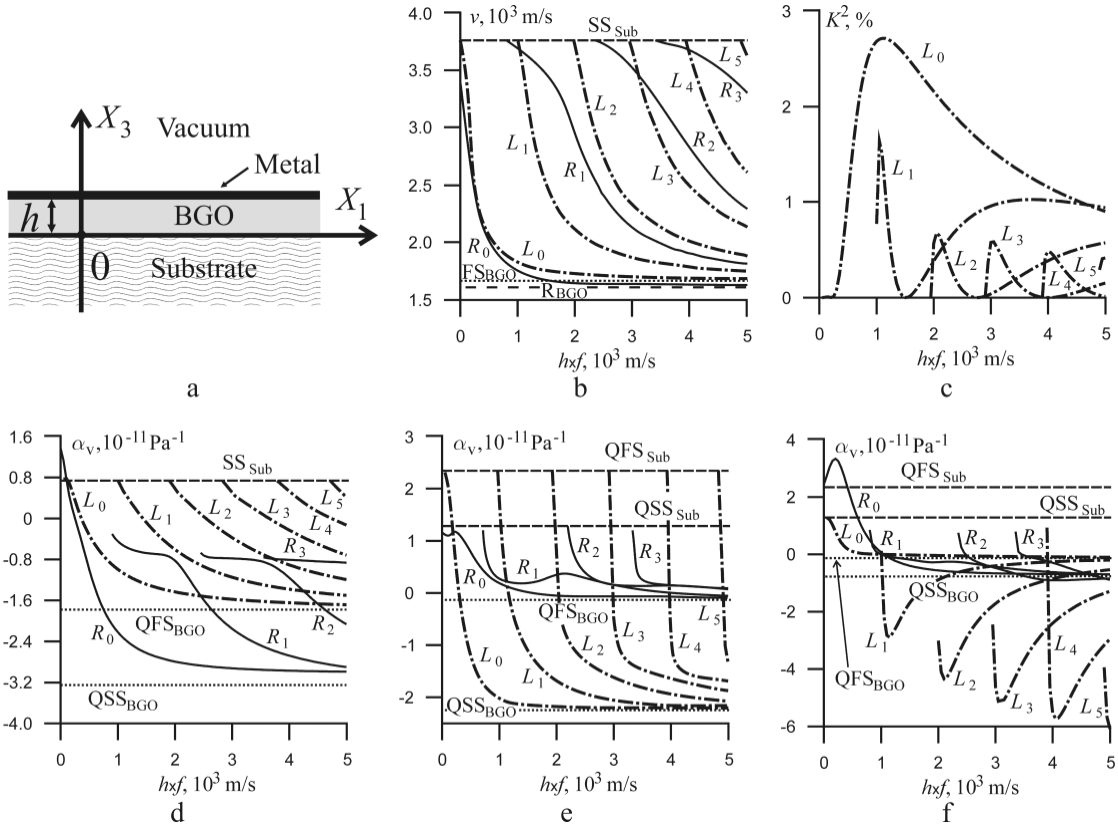

Fig. 1. Dispersion relations for acoustic wave propagation in "[100](001) BGO/fused silica" layered structure: (a) — configuration of layered piezoelectric structure; (b) — phase velocities; (c) — EMCC at $z = h$; (d) — α_v coefficients in the case of $P \parallel X_1$; (e) — α_v coefficients in the case of $P \parallel X_2$; (f) — α_v coefficients in the case of $P \parallel X_3$. QSS_{BGO}, QSS_{Sub}, QFS_{BGO} and QFS_{Sub} are the slow bulk acoustic wave and fast quasishear wave in the layer and substrate, respectively. R_i and L_i are the ith order modes of Rayleigh and Love waves, respectively

for BGO (Fig. 1, b). The velocity of zero-order mode of Rayleigh wave tends to Rayleigh SAW velocity of BGO in the given propagation direction (1625.92 m/s) as parameter $h \times f$ increases. The piezoelecric activity is observed for pure modes of Love wave. The calculation of EMCC was performed in the case of metalization of the upper side of piezoelectric layer ($z = h$). The maximum value of $K^2 = 2.71\%$ is observed at $h \times f = 1100$ m/s for the zero-order mode of Love wave (Fig. 1, c). It should be noted that in any discussed variant of pressure direction the modes of elastic wave remain pure modes, in contrast to the case of dc electric field application.

When pressure $P \parallel X_1$ acts on the layered structure as a whole the shear bulk wave in BGO is split into fast and slow bulk shear waves. As mentioned above (9), bulk shear wave in the fused silica remain to be degenerative wave (Fig. 1, d). With increasing parameter $h \times f$ the coefficients α_v of the Rayleigh waves is varied from the value $\alpha_v = 1.37 \cdot 10^{-11}\,\mathrm{Pa}^{-1}$ observed for the mode R_0 to the value ($\alpha_v = -3.253 \cdot 10^{-11}\,\mathrm{Pa}^{-1}$) observed for the slow shear wave in BGO. The α_v values of the Love wave modes decrease gradually from $\alpha_v = 7.399 \cdot 10^{-12}\,\mathrm{Pa}^{-1}$ for the shear wave of fused silica to $\alpha_v = -1.78 \cdot 10^{-11}\,\mathrm{Pa}^{-1}$ for the fast shear wave in BGO.

When pressure $P \parallel X_2$ the shear bulk wave as in BGO and in fused silica is split into fast

and slow waves (Fig. 1, e). With increasing parameter $h \times f$ the values of α_v of Rayleigh wave modes are varied from $\alpha_v = 1.28 \cdot 10^{-11}\,\mathrm{Pa}^{-1}$ observed for the shear wave of fused silica to $\alpha_v = -1.33 \cdot 10^{-12}\,\mathrm{Pa}^{-1}$ observed for the fast shear wave in BGO. The values of α_v of the Love wave modes decrease gradually from $\alpha_v = 2.35 \cdot 10^{-11}\,\mathrm{Pa}^{-1}$ observed for the fast shear wave in fused silica to $\alpha_v = -2.25 \cdot 10^{-11}\,\mathrm{Pa}^{-1}$ observed for the slow shear wave in BGO.

When pressure $P \parallel X_3$ the splitting of bulk acoustic shear wave as in BGO and in fused silica also occurs with the generation of fast and slow shear waves (Fig. 1, f). With increasing parameter $h \times f$ the values of α_v of Rayleigh wave modes are varied $\alpha_v = 2.35 \cdot 10^{-11}\,\mathrm{Pa}^{-1}$ observed for the shear wave in fused silica to $\alpha_v = -7.764 \cdot 10^{-12}\,\mathrm{Pa}^{-1}$ observed for the slow shear wave in BGO. The values of α_v of the Love wave modes decrease gradually from $\alpha_v = 1.28 \cdot 10^{-11}\,\mathrm{Pa}^{-1}$ observed for the slow shear wave then they reach a minimum and go to $\alpha_v = -1.33 \cdot 10^{-12}\,\mathrm{Pa}^{-1}$ observed for the fast shear wave in BGO.

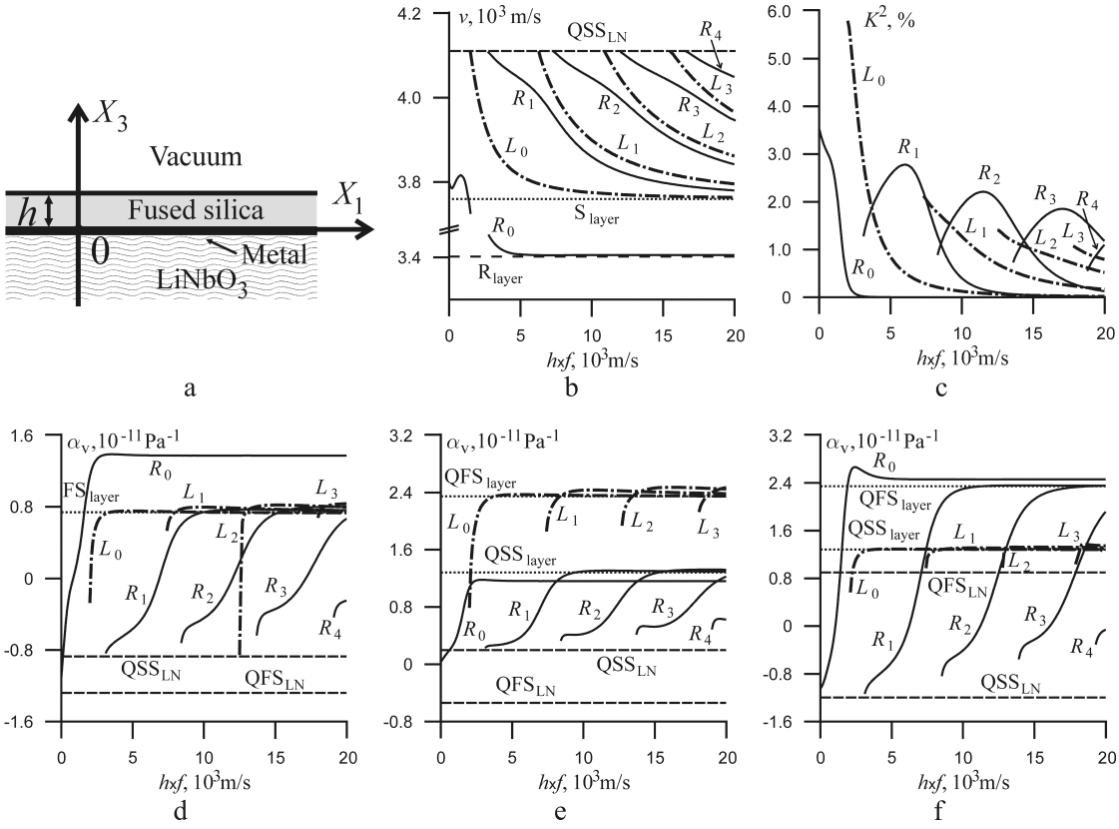

Fig. 2. Dispersion relations for acoustic wave propagation in "fused silica/[010](100)$LiNbO_3$" layered structure: (a) — configuration of layered piezoelectric structure; (b) — phase velocities; (c) — EMCC at $z = 0$; (d) — α_v coefficients in the case of $P \parallel X_1$; (e) — α_v coefficients in the case of $P \parallel X_2$; (f) — α_v coefficients in the case of $P \parallel X_3$. QSS_{layer}, QSS_{LN}, QFS_{layer}, and QFS_{LN} are the slow bulk acoustic and fast quasi-shear waves in the layer and substrate, respectively. R_{layer} denotes the Rayleigh wave in the layer. R_i and L_i are the i^{th}-order modes of Rayleigh and Love waves, respectively

Dispersion relations for the phase velocity, the EMCC and coefficients α_v for the Rayleigh and Love waves in the "fused silica/[010](100) LN" structure are presented in Fig. 2. Parameter

$h \times f$ is in range from 0 to 20000 m/s. The Love wave phase velocities is varied from the values of the LN shear wave phase velocity to the shear wave phase velocity in fused silica (Fig. 2, b). The Rayleigh wave velocity tends to the Rayleigh SAW velocity in fused silica in a given propagation direction (3405.5 m/s) as parameter $h \times f$ increases. There are no pure modes in this structure because the EMCC coefficients are not equal to zero for all modes of Rayleigh and Love waves. The calculation of EMCC was performed for metallized "layer/substrate" interface ($z = 0$). The maximum value of $K^2 = 5.79$ % is observed at $h \times f = 2000$ m/s for the zero-order mode of the Love wave (Fig. 2, c).

When pressure $P \parallel X_1$ the fast and slow shear bulk waves propagate in LN as in undisturbed crystal. The bulk shear wave in fused silica remains to be degenerative wave but the value of its phase velocity is changed (Fig. 2, d). With increasing parameter $h \times f$ coefficients α_v of the mode R_0 are varied from the initial value $\alpha_v = -1.11 \cdot 10^{-11}\,\mathrm{Pa}^{-1}$ to $\alpha_v = 1.39 \cdot 10^{-11}\,\mathrm{Pa}^{-1}$ at $h \times f = 3500$ m/s. With increasing parameter $h \times f$ coefficients α_v of higher-order modes of Rayleigh and Love waves vary from $\alpha_v = -8.72 \cdot 10^{-12}\,\mathrm{Pa}^{-1}$ for the LN bulk slow shear wave to $\alpha_v = 7.4 \cdot 10^{-12}\,\mathrm{Pa}^{-1}$ for the bulk shear wave of fused silica.

When pressure $P \parallel X_2$ the bulk shear waves in both the layer and substrate is split into the fast and slow waves (Fig. 2, e). With increasing parameter $h \times f$ coefficients α_v of the modes of Rayleigh wave, except the mode R_0, are varied from $\alpha_v = 1.98 \cdot 10^{-12}\,\mathrm{Pa}^{-1}$ for the LN bulk slow shear wave to $\alpha_v = 1.28 \cdot 10^{-11}\,\mathrm{Pa}^{-1}$ for the bulk slow shear wave in fused silica. The values of α_v of the modes of Love wave increase gradually to $\alpha_v = 2.35 \cdot 10^{-11}\,\mathrm{Pa}^{-1}$ for the bulk fast shear wave in fused silica.

When pressure $P \parallel X_3$ the splitting of both the layer and substrate bulk acoustic shear waves occurs with the generation of fast and slow shear waves (Fig. 2, f). With increasing parameter $h \times f$ coefficients α_v of the modes of Rayleigh wave are varied from $\alpha_v = -1.198 \cdot 10^{-11}\,\mathrm{Pa}^{-1}$ for the LN bulk slow shear wave to $\alpha_v = -2.35 \cdot 10^{-11}\,\mathrm{Pa}^{-1}$ for the bulk fast shear wave in fused silica. The values of α_v of the modes of Love wave tend to $\alpha_v = 1.28 \cdot 10^{-11}\,\mathrm{Pa}^{-1}$ for the bulk slow shear wave in fused silica.

Some results on the maximal coefficients α_v as well as data on phase velocities and EMCC for the piezoactive modes of Rayleigh and Love waves are presented in Table 1 in the case when uniaxial pressure is simultaneously applied to the layer and substrate (Tab. 1).

Table 1. Data on the parameters of acoustic waves in layered structures with the maximal coefficients α_v and non-zero EMCC values

Structure	Mode	Phase velocity (m/s)	K^2 (%)	$h \times f$ (m/s)	α_v, 10^{-11} Pa^{-1}		
					$P \parallel X_1$	$P \parallel X_2$	$P \parallel X_3$
[100](001)	L_0	1683.38	0.9	5000	-1.68	-2.20	-0.10
"BGO/fused silica"	L_0	3630.14	0.01	50	0.77	2.31	1.28
	L_5	3617.53	0.4	5000	0.41	-1.34	-6.08
[010](100)	R_0	3418.85	0.007*	3600	1.39	1.17	2.53
"fused silica/LN"	L_3	3968.96	0.8*	20000	0.84	2.47	1.35
	R_0	3496.23	0.1*	2400	1.31	1.16	2.67

* EMCC calculated at z=0

Fig. 3 shows the anisotropy of the Rayleigh and Love wave parameters for the "(001) BGO/fused silica" structure under various uniaxial pressure directions and for three values of the parameter $h \times f = 500$, 1500, and 2500 m/s.

The angle ψ defines the wave propagation direction and it was varied from [100] to [010] direction of BGO. At $h \times f = 2500$ m/s the hybridization between R_1 и L_1 modes is observed

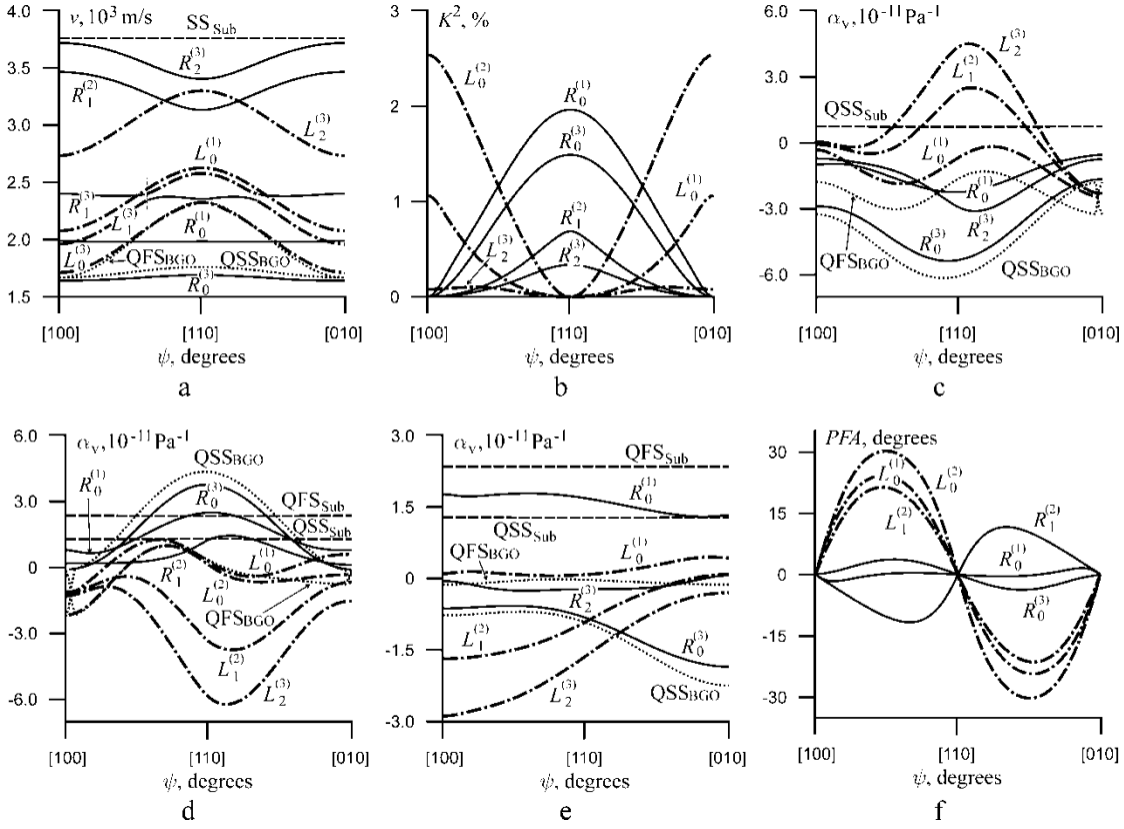

Fig. 3. Anisotropy of acoustic waves parameters in a layered structure "(001) BGO/fused silica" for three values of $h \times f$ (m/s) (1) — 500, (2) — 1500, (3) — 2500: (a) — phase velocities; (b) — EMCC calculated at $z = h$; (c) — coefficients α_v in the case of $P \parallel X_1$; (d) — coefficients α_v in the case of $P \parallel X_2$; (e) — coefficients α_v in the case of $P \parallel X_3$; (f) — PFA. Curves specified as QSS_{BGO}, QSS_{Sub}, QFS_{BGO} and QFS_{Sub} are associated with bulk acoustic slow and fast shear waves in the layer and substrate, respectively. Curves specified as R_i и L_i are related to the modes of Rayleigh and Love waves, respectively. Configuration of the layered structure is shown in Fig. 1, a

when the angle ψ is varied from 28° to 62°. Hybridization areas are marked by the vertical dashed lines (Fig. 3, a). The generalized modes of Rayleigh and Love waves propagate in the plane and both wave types have significant piezoelectric activity. Zero-order mode of the Love wave has the maximum value of $K^2 = 2.54$ % at $h \times f = 1500$ m/s in the [100] wave propagation direction. Zero-order mode of the Rayleigh wave has the maximum value of $K^2 = 1.96$ % at $h \times f = 500$ m/s and $\psi = 45°$ (Fig. 3, b). In the case $P \parallel X_1$ the maximum value of $\alpha_v = -5.37 \cdot 10^{-11}\,\mathrm{Pa}^{-1}$ is observed for the mode R_0 at $h \times f = 2500$ m/s and ψ=42° (Fig. 3, c). When $P \parallel X_2$ the maximum value of $\alpha_v = -6.22 \cdot 10^{-11}\,\mathrm{Pa}^{-1}$ is observed for the mode L_2 at $h \times f = 2500$ m/s and $\psi = 51°$ (Fig. 3, d). When pressure $P \parallel X_3$ the maximum value of $\alpha_v = -2.88 \cdot 10^{-11}\,\mathrm{Pa}^{-1}$ is also observed for the mode L_2 at $h \times f = 2500$ m/s and $\psi = 0°$ (Fig. 3, e). Note that the values of α_v have the same order of magnitude for all chosen directions of pressure P. Anisotropy of the coefficients α_v for the Love and Rayleigh modes is similar to the anisotropy observed for fast and slow shear bulk acoustic waves in BGO, respectively. However, both the shear bulk acoustic

waves in fused silica substrate show weak anisotropy and the difference between coefficients α_v at $\psi = 0°$ and $\psi = 45°$ is about 10^{-13} Pa^{-1}. The angles of the energy power flow (PFA) were calculated for zero-order and first-order modes (Fig. 3, f). The given crystalline cut can be characterized by considerable anisotropy of phase velocity and, therefore, one can find the sectors with large PFA values. Thus, the maximum value of the PFA equal to 30.2° is observed for the mode L_0 when $h \times f = 1500$ m/s and $\psi = 22°$. The maximum value of the PFA=–11.7° is observed for the mode R_0 at $h \times f = 1500$ m/s and $\psi = 30°$.

Table 2 shows the characteristics of the elastic wave modes propagating in the structure "(001) BGO/fused silica" with the maximum values of the coefficients α_v.

Table 2. Anisotropy of acoustic waves parameters in the "(001) BGO/fused silica" layered structure

Mode	Angle ψ (degrees)	Phase velocity (m/s)	$h \times f$ (m/s)	K^2 (%)	PFA (degrees)	α_v, 10^{-11} (Pa^{-1})		
						$P \parallel X_1$	$P \parallel X_2$	$P \parallel X_3$
L_2	48	3293.84	2500	0.002	-4.52	4.5	-6.16	-1.49
R_0	42	1690.16	2500	1.48	0.85	-5.37	3.72	-0.76
L_2	51	3274.46	2500	0.006	-8.47	4.39	-6.22	-1.35
R_0	46	1690.75	2500	1.49	-0.28	-5.29	3.75	-0.85
L_2	0	2734.08	2500	0.08	0	0.04	-1.29	-2.88
R_0	90	1641.10	2500	0	0	-1.65	-0.14	-1.85

Conclusion

Basic equations and boundary conditions describing the propagation of acoustic waves in piezoelectric layered structures subjected to uniform pressure have been obtained. The propagation of dispersive acoustic modes in the "[100](001) BGO/fused silica" and "fused silica/[010](100) $LiNbO_3$" layered structures has been analyzed in detail. Selection of solutions identified as the various order modes of Rayleigh and Love waves has been fulfilled. Dispersion relations for the phase velocity, EMCC and coefficients α_v as a function of the parameter $h \times f$ have been calculated. Anisotropy of acoustic wave parameters in the "(001)BGO/fused silica" structure has been investigated. Cuts and directions with the extreme values of the coefficients α_v have been found for a number of acoustic modes. It should be noted that the values of the coefficients α_v for dispersive Rayleigh modes in the layered structure are strictly between the corresponding values of the coefficients α_v for the slow shear waves in the layer and the substrate. Thus, the highest values of the coefficients α_v should be expected in the vicinity of the direction of the acoustic axis of the substrate when the degeneracy is removed under the influence of given pressure.

This research was supported by the Russian Federation Program for Supporting Scientific Schools under grant no.4828.2012.2.

References

[1] R.J.Meyer, T.C.Montgomery, W.J.Hughes, Tonpilz transducers designed using single crystal piezoelectrics, *Oceans '02 MTS/IEEE* (Biloxi, Mississippi, USA), **4**(2002), 2328–2333.

[2] S.Lee, D.L.Pei, Y.Roh, Optimal design of a 1–3 piezocomposite tonpilz transducer by means of the finite element method, *Proc. IEEE Ultrasonics Symp.* (Vancouver, Canada), 2006, 1521–1524.

[3] K.A.Snook, P.W.Rehrig, W.S.Hackenberger, R.J.Meyer, D.Markley, Tailored single crystal orientations for improved tonpilz transducer performance, *Proc. IEEE Ultrasonics Symp.* (Vancouver, Canada), 2006, 359–362.

[4] F.Kubat, W.Ruile, T.Hesjedal, J.Stotz, U.Rösler, L.M. Reindl, Calculation and experimental verification of the acoustic stress at GHZ frequencies in SAW resonators, *IEEE Trans. on Ultrason., Ferroel. and Freq. Control*, **51**(2004), no. 11, 1437–1448.

[5] Y.Jing, J.Chen, X.Gong, J.Duan, Stress-induced frequency shifts in rotated Y-cut langasite resonators with electrodes considered, *IEEE Trans. on Ultrason., Ferroel. and Freq. Control*, **54**(2007), no. 5, 906–909.

[6] J.A.Kosinski, R.A.Pastore, Jr., J.Yang, X.Yang, J.A.Turner, Stress-induced frequency shifts of degenerate thickness-shear modes in rotated Y-cut quartz resonators, *IEEE Trans. on Ultrason., Ferroel. and Freq. Control*, **57**(2010), no. 8, 1880–1883.

[7] J.A.Kosinski, R.A.Pastore Jr., X.Yang, J.Yang, J.A.Turner, Stress-induced frequency shifts in langasite thickness-mode resonators, *IEEE Trans. on Ultrason., Ferroel. and Freq. Control*, **59**(2009), no. 1, 129–135.

[8] H.Zhang, J.A.Kosinski, Analysis of contributions of nonlinear material constants to stress-induced velocity shifts of quartz and langasite surface acoustic wave resonators, *IEEE Trans. on Ultrason., Ferroel. and Freq. Control*, **60**(2013), no. 5, 975–985.

[9] S.I.Burkov, B.P.Sorokin, K.S.Aleksandrov, A.A.Karpovich, Reflection and refraction of bulk acoustic waves in piezoelectrics under uniaxial stress, *Acoustical Physics*, **55**(2009), no. 2, 178–185.

[10] S.I.Burkov, B.P.Sorokin, A.A.Karpovich, K.S.Aleksandrov, Reflection and refraction of bulk acoustic waves in piezoelectric crystals under the action of bias electric field and uniaxial pressure, *Proc. IEEE Ultrasonics Symp.* (Beijing, China), 2008, 2161–2164.

[11] H.Liu, Z.K.Wang, T.J.Wang, Effect of initial stress on the propagation behavior of Love waves in a layered piezoelectric structure, *Int. J. of Solids and Structures*, **38**(2001), 37–51.

[12] Z.H.Qian, F.Jin, Z.K.Wang, K.Kishimoto, Love waves propagation in a piezoelectric layered structure with initial stresses, *Acta Mech.*, **171**(2004), 41–57.

[13] Z.H.Qian, F.Jin, T.Lu, K.Kishimoto, S.Hirose, Effect of initial stress on Love waves in a piezoelectric structure carrying a functionally graded material layer, *Ultrasonics*, **50**(2010), 84–90.

[14] K.S.Aleksandrov, B.P.Sorokin, S.I.Burkov, Effective piezoelectric crystals for acoustoelectronics, piezotechnics and sensors, vol. 2, Novosibirsk, SB RAS Publishing House, 2008 (in Russian).

[15] M.P.Zaitseva, Yu.I.Kokorin, Yu.M.Sandler, V.M.Zrazhevsky, B.P.Sorokin, A.M.Sysoev, Non-linear electromechanical properties of acentric crystals, Novosibirsk, Nauka, 1986 (in Russian).

[16] S.I.Burkov, B.P.Sorokin, A.A.Karpovich, K.S.Aleksandrov, The influence of static homogeneous fields on the properties of SAW in piezoelectrics, *Ferroelectrics Letters*, **14**(1992), no. 5/6, 99–113.

[17] B.P.Sorokin, M.P.Zaitseva, Yu.I.Kokorin, S.I.Burkov, B.V.Sobolev, N.A.Chetvergov, Anisotropy of the bulk acoustic wave velocity under the electric field in the sillenite structure piezoelectric crystals, *Soviet Fiz. Acoust.*, **32**(1986), no. 5, 664–666 (in Russian).

[18] Yu.I.Kokorin, B.P.Sorokin, S.I.Burkov, K.S.Aleksandrov, Changes of acoustic properties of a cubic piezoelectric crystal in the presence of constant electric field, *Sov. Kristallographiya*, **31**(1986), no. 4, 706–709 (in Russian).

[19] Y.Cho, K.Yamanouchi, Nonlinear, elastic, piezoelectric, electrostrictive, and dielectric constants of lithium niobate, *J. Appl. Phys.*, **61**(1987), no. 3, 875–887.

[20] H.J.McSkimin, Measurement of elastic constants at low temperatures by means of ultrasonic waves–data for silicon and germanium single crystals, and for fused silica, *J. Appl. Phys.*, **24**(1953), 988–997.

[21] S.I.Burkov, O.P.Zolotova, B.P.Sorokin, Influence of bias electric field on elastic waves propagation in piezoelectric layered structures, *Ultrasonics*, **53**(2013), no. 6, 1059–1064.

[22] S.I.Burkov, O.P.Zolotova, B.P.Sorokin, Calculation of the dispersive characteristics of acoustic waves in piezoelectric layered structures under the effect of dc electric field, *IEEE Trans. on Ultrason., Ferroel. and Freq. Control*, **59**(2012), no. 10, 2331–2337.

Влияние однородного давления на распространение акустических волн в пьезоэлектрических слоистых структурах

Сергей И. Бурков
Ольга П. Золотова
Борис П. Сорокин

Получены основные уравнения и граничные условия для описания распространения акустических волн в пьезоэлектрических слоистых структурах в условиях действия одноосного давления. Рассчитаны дисперсионные зависимости фазовых скоростей, КЭМС, коэффициентов управляемости как функций от параметра $h \times f$ в пьезоэлектрических слоистых структурах „[100](001) BGO/плавленый кварц“ и „плавленый кварц/[010](100) $LiNbO_3$“. Исследована анизотропия параметров распространения акустических волн в структуре (001) „BGO/плавленый кварц“. Определены срезы и направления распространения волн с экстремальными значениями коэффициентов управляемости.

Ключевые слова: пьезоэлектрическая слоистая структура, волна Лява, волна Рэлея, одноосное давление.